



Crystal structure of dicaesium strontium hexacyanidoferrate(II), $\text{Cs}_2\text{Sr}[\text{Fe}(\text{CN})_6]$, from laboratory X-ray powder data

Nicolas Massoni,^{a*} Mícheál P. Moloney,^a Agnès Grandjean,^a Scott T. Misture^b and Hans-Conrad zur Loye^c

Received 15 April 2020

Accepted 18 May 2020

Edited by M. Weil, Vienna University of Technology, Austria

Keywords: crystal structure; X-ray powder diffraction; caesium strontium hexaferrocyanate; cryolite-type structure.

CCDC reference: 2004551

Supporting information: this article has supporting information at journals.iucr.org/e

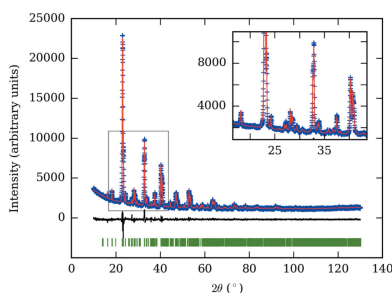
^aCEA, DES, ISEC, DE2D, Univ Montpellier, Marcoule, France, ^bKazuo Inamori School of Engineering, Alfred University, Alfred, NY, 14802, USA, and ^cCenter for Hierarchical Waste Form Materials, Columbia, SC, 29208, USA.

*Correspondence e-mail: nicolas.massoni@cea.fr

Ferrocyanides with general formula $A^I_xB^{II}_y[\text{Fe}(\text{CN})_6]$, where A and B are cations, are thought to accept many substitutions on the A and B positions. In this communication, the synthesis and crystal structure of $\text{Cs}_2\text{Sr}[\text{Fe}(\text{CN})_6]$ are reported. The latter was obtained from $\text{K}_2\text{Ba}[\text{Fe}(\text{CN})_6]$ particles, put in contact with caesium and strontium ions. Hence, a simultaneous ion-exchange mechanism (Cs for K, Sr for Ba) occurs to yield $\text{Cs}_2\text{Sr}[\text{Fe}(\text{CN})_6]$. The synthesis protocol shows that $\text{K}_2\text{Ba}[\text{Fe}(\text{CN})_6]$ particles can be used for the simultaneous trapping of radioactive caesium and strontium nuclides in water streams. $\text{Cs}_2\text{Sr}[\text{Fe}(\text{CN})_6]$ adopts the cryolite structure type and is isotypic with the known compound $\text{Cs}_2\text{Na}[\text{Mn}(\text{CN})_6]$ [dicaesium sodium hexacyanidomanganate(III)]. The octahedrally coordinated Sr and Fe sites both are located on inversion centres, and the eightfold-coordinated Cs site on a general position.

1. Chemical context

Ferrocyanides (FCN), such as Prussian blue, were discovered almost 300 years ago. The attractive properties of these materials for batteries and decontamination processes have ensured that FCNs remain an active research topic (Haas, 1993; Paoletta *et al.*, 2017). In particular, potassium copper FCN is currently being investigated for the purification of ^{137}Cs -contaminated water streams through partial exchange with potassium (Haas, 1993; Mimura *et al.*, 1997). To the best of our knowledge, however, using FCNs to extract strontium either alone or with caesium has never been considered before. In the framework of the Center for Hierarchical Waste Forms (CHWM), an Energy Frontier Research Center (EFRC) funded by the US Department of Energy, we have been working on potassium copper FCN as an efficient K-ionic exchanger to capture ^{137}Cs and serve as a waste containment matrix (zur Loye *et al.*, 2018). In this context, we have synthesized a caesium strontium FCN to study its efficiency in immobilizing both ^{90}Sr and ^{137}Cs , two radionuclides that are in most cases found together in radioactive water streams. Caesium strontium FCNs appear to be poorly described in the ICDD 2020 PDF4+ powder diffraction database (Gates-Rector & Blanton, 2019). Since the synthesized phase $\text{Cs}_2\text{Sr}[\text{Fe}(\text{CN})_6]$ did not match with existing entries, we decided to characterize the structure and we report the results herein.



OPEN ACCESS

Table 1

 Comparison of lattice parameters (Å, °), selected bond lengths (Å) and volumes (Å³) for Cs₂Sr[Fe(CN)₆] and Cs₂Na[Mn(CN)₆].

	Cs ₂ Sr[Fe(CN) ₆]		Cs ₂ Na[Mn(CN) ₆]
<i>a</i> , <i>b</i> , <i>c</i>	7.6237 (2), 7.7885 (2), 10.9600 (3)	<i>a</i> , <i>b</i> , <i>c</i>	7.597 (1), 7.806 (1), 10.950 (1)
α , β , γ	90, 90.4165 (19), 90	α , β , γ	90, 90.07 (1), 90
<i>V</i>	650.76 (4)	<i>V</i>	649.36
Cs polyhedron volume*	44.56	Cs polyhedron volume*	44.46
Cs—C1	3.603 (4)	Cs—C1	3.6291 (5)
Cs—N1	3.348 (4)	Cs—N1	3.3688 (5)
Cs—C1 ⁱ	3.628 (3)	Cs—C1 ⁱ	3.5936 (5)
Cs—N1 ⁱ	3.5232 (18)	Cs—N1 ⁱ	3.4920 (5)
Cs—C2 ⁱⁱ	3.592 (6)	Cs—C2 ⁱⁱ	3.5831 (4)
Cs—N2 ⁱⁱ	3.367 (6)	Cs—N2 ⁱⁱ	3.3839 (3)
Cs—C3 ⁱⁱⁱ	3.711 (5)	Cs—C3 ⁱⁱⁱ	3.7044 (4)
Cs—N3 ⁱⁱⁱ	3.274 (6)	Cs—N3 ⁱⁱⁱ	3.2840 (3)
Sr octahedron volume*	20.49	Na octahedron volume*	20.45
Fe octahedron volume*	10.49	Mn octahedron volume*	10.47

*Atomic bond lengths were not compared since the positions of C, N, Fe and Sr were not refined. Volumes were calculated by VESTA V3.2.1 (Momma & Izumi, 2011). [Symmetry codes: (i) $-x + \frac{1}{2}, y - \frac{1}{2}, -z + \frac{1}{2}$; (ii) $x + 1, y, z$; (iii) $x + \frac{1}{2}, -y + \frac{1}{2}, z + \frac{1}{2}$]

2. Structural commentary

Cs₂Sr[Fe(CN)₆] is isotypic with Cs₂Na[Mn(CN)₆] (Ziegler *et al.*, 1989). As shown in Table 1, the lattice parameters of Cs₂Sr[Fe(CN)₆] are slightly greater than those of Cs₂Na[Mn(CN)₆], but the cell volumes differ by less than 0.3%. The crystal structure adopts the cryolite structure type and comprises a framework of corner-sharing [Sr(CN)₆] (dark green in Fig. 1) and [Fe(CN)₆] octahedra (brown in Fig. 1). Both types of octahedra exhibit site symmetry $\bar{1}$, with Sr situated on Wyckoff position 2 *c*, and Fe on 2 *a*. In the voids of this framework, Cs sites (light green in Fig. 1) have a distorted square-antiprismatic environment with four C and four N atoms as ligands. The substitution of manganese by iron in

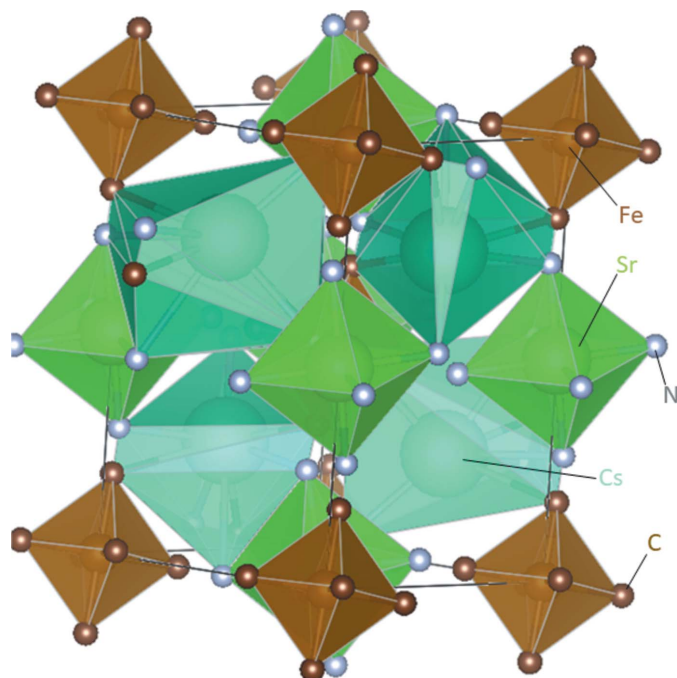


Figure 1
Polyhedral plot of the cryolite-type Cs₂Sr[Fe(CN)₆] crystal structure.

Cs₂Na[Mn(CN)₆] can be explained by the similar ionic radii of the two elements: $r_{\text{Mn(III)}} = 0.58 \text{ \AA}$ and $r_{\text{Fe(II)}} = 0.61 \text{ \AA}$ (Shannon, 1976). For the substitution of sodium by strontium, the ionic radii differ more substantially: $r_{\text{Na(I)}} = 1.02 \text{ \AA}$ and $r_{\text{Sr(II)}} = 1.18 \text{ \AA}$. The two crystal structures were compared numerically using COMPSTRU (de la Flor *et al.*, 2016). The structure similarity index Δ was calculated to be 0.009 (Bergerhoff *et al.*, 1999). However, since only a few parameters (11) were refined and many parameters kept fixed in the refinement, the similarity index is not reliable.

3. Database survey

Ferrocyanides have rather complex structures. The ICDD 2020 PDF4+ database (Gates-Rector & Blanton, 2019) contains records of about 1521 phases with the general $A^1_x B^{II}_y [\text{Fe}(\text{CN})_6]$ ferrocyanide formula in which *A* and *B* are cations, with no constraints on the *A*:*B* ratio. As shown in

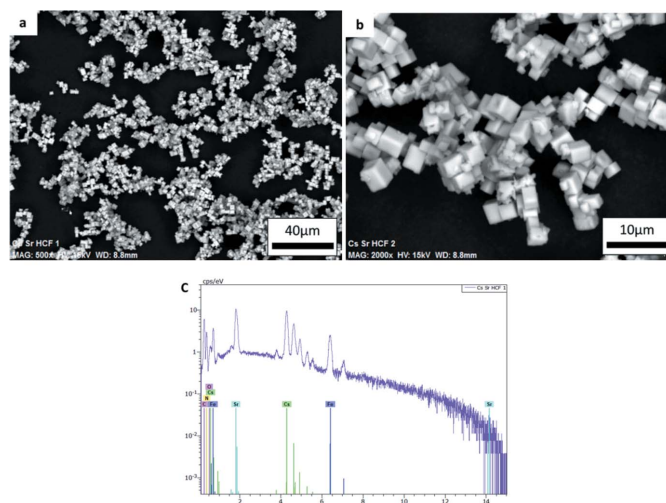
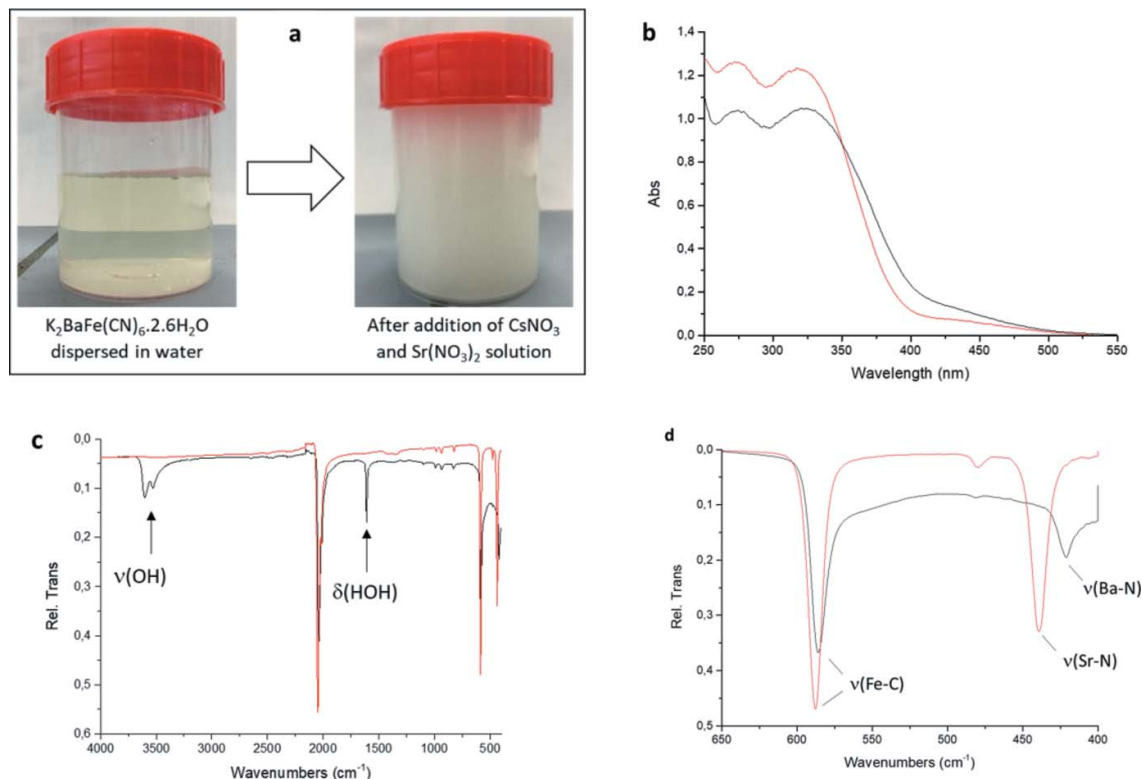


Figure 2
(*a*) and (*b*) SEM-backscattered electron images of Cs₂Sr[Fe(CN)₆]. (*c*) EDS spectrum of Cs₂Sr[Fe(CN)₆].


Figure 3

(a) Pictures of a clear yellow $\text{K}_2\text{Ba}[\text{Fe}(\text{CN})_6]\cdot 2.6\text{H}_2\text{O}$ dispersion before (left) and immediately after (right) the addition of Cs/Sr. (b) UV-Vis spectra of $\text{K}_2\text{Ba}[\text{Fe}(\text{CN})_6]\cdot 2.6\text{H}_2\text{O}$ (black) and $\text{Cs}_2\text{Sr}[\text{Fe}(\text{CN})_6]$ (red). Both spectra show the characteristic features of the $[\text{Fe}(\text{CN})_6]$ moiety (Gray & Beach, 1963). (c) FT-IR spectra of K_2BaHCF (black) and Cs_2SrHCF (red). All peaks shift to higher frequencies after ion exchange. The arrows indicate the $\delta(\text{HOH})$ signal at 1611 cm^{-1} and $\nu(\text{OH})$ signals at 3527 cm^{-1} and 3601 cm^{-1} observed for K_2BaHCF but not for Cs_2SrHCF . These signals indicate the presence of structural water, which is common in hexacyanidoferrate particles. (d) Enlarged view of the FT-IR spectra in the $400\text{--}650\text{ cm}^{-1}$ range.

Fig. 2, the studied sample contained only Cs, Sr, Fe, C and N. Hence, we focused on ferrocyanides with $A^{\text{I}} = \text{Cs}$ and $B^{\text{II}} = \text{Sr}$, for which only three phases have been reported, however with poorly described crystal data. The $\text{Cs}_2\text{Sr}[\text{Fe}(\text{CN})_6]$ phase studied by Kuznetsov *et al.* (1970) is reported to crystallize in the tetragonal crystal system with a ranging from 10.72 to 10.89 Å and c from 10.75 to 10.99 Å (PDF00-024-0293 and PDF00-24-0294). The entry for the third phase (PDF00-048-1203), the hydrated ferrocyanide $\text{CsSr}[\text{Fe}(\text{CN})_6]\cdot 3\text{H}_2\text{O}$ reported by Slivko *et al.* (1988), is comprised only of reflections without further crystal data given. None of these PDF cards matched the X-ray diffraction pattern of the studied sample. As shown in Fig. 2*a,b*, the cubic crystal habit revealed by SEM measurements hints at a crystal structure with cubic symmetry, but the number of reflections is not consistent with such a highly symmetrical crystal system. The whole pattern can be described by a monoclinic cell and the experimental data are well reproduced by adjusting the reflections from the $\text{Cs}_2\text{Na}[\text{Mn}(\text{CN})_6]$ phase (Ziegler *et al.*, 1989; PDF 04-012-3126). The $\text{Cs}_2\text{Sr}[\text{Fe}(\text{CN})_6]$ crystal structure was refined from that of $\text{Cs}_2\text{Na}[\text{Mn}(\text{CN})_6]$ assuming complete substitution of manganese by iron and sodium by strontium. As described above, the ionic radii of the corresponding metals are close enough for these substitutions to be possible.

4. Synthesis and crystallization

All solutions were prepared using Millipore water. $\text{Cs}_2\text{Sr}[\text{Fe}(\text{CN})_6]$ (Cs_2SrHCF) particles were not prepared directly by adding Sr and Cs salts to $\text{K}_4[\text{Fe}(\text{CN})_6]\cdot 3\text{H}_2\text{O}$. Although it was found that Cs_2SrHCF could be prepared directly by adding aqueous $\text{Sr}(\text{NO}_3)_2$ to a $\text{K}_4[\text{Fe}(\text{CN})_6]\cdot 3\text{H}_2\text{O}/\text{CsNO}_3$ solution, the yield was extremely poor ($\leq 1\%$). Instead, an ion-exchange reaction was initiated by adding a mixed $\text{Sr}(\text{NO}_3)_2/\text{CsNO}_3$ solution to $\text{K}_2\text{Ba}[\text{Fe}(\text{CN})_6]$ particles, thereby simultaneously substituting barium for strontium and potassium for cesium. This simple approach, using $\text{K}_2\text{Ba}[\text{Fe}(\text{CN})_6]\cdot 2.6\text{H}_2\text{O}$ (K_2BaHCF) as an intermediate compound, allowed 1:1 amounts of Cs_2SrHCF to be produced from K_2BaHCF by ion exchange.

Briefly, the K_2BaHCF itself was prepared by adding a 1.5 M solution of $\text{Ba}(\text{NO}_3)_2$ to a 1 M solution of $\text{K}_4[\text{Fe}(\text{CN})_6]\cdot 3\text{H}_2\text{O}$ as described by Padigi *et al.* (2015). Once prepared, K_2BaHCF was collected by centrifugation, washed and dried. Its chemical composition (K, Fe and Ba) and water content, respectively, were determined by inductively coupled plasma (ICP) analysis and thermogravimetric analysis (TGA). The dried K_2BaHCF particles redispersed readily in water, producing a clear, slightly yellow dispersion. Cs_2SrHCF forms immediately as a milky white precipitate (Fig. 3*a*) upon adding

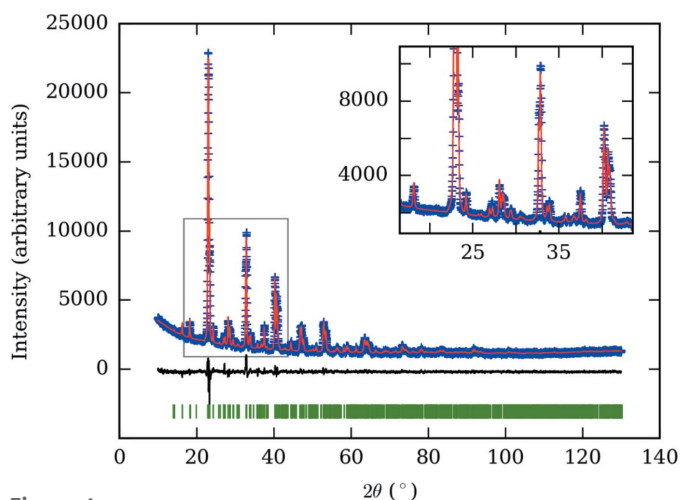


Figure 4 Observed and calculated X-ray powder diffraction intensities for $\text{Cs}_2\text{Sr}[\text{Fe}(\text{CN})_6]$.

the mixed $\text{CsNO}_3/\text{Sr}(\text{NO}_3)_2$ solution to the clear yellow K_2BaHCF dispersion. To ensure complete substitution, 2.2 moles of CsNO_3 and 1.1 moles of $\text{Sr}(\text{NO}_3)_2$ were added for every mole of K_2BaHCF present. After being left to mix for 1 h, the formed Cs_2SrHCF was collected by centrifugation, washed and dried. The chemical composition (Fe and Sr) of the powder was determined by ICP analysis while the Cs content was determined by atomic absorption spectroscopy (AAS). An initial characterization of the Cs_2SrHCF powder was carried out by TGA, UV–Vis and FT–IR spectroscopy. The UV–Vis spectrum of the Cs_2SrHCF (Fig. 3*b*) confirmed that the $[\text{Fe}(\text{CN})_6]$ moiety was maintained with only slight decreases in the wavelengths of the various absorption peaks (Gray & Beach, 1963). The FT–IR spectra of Cs_2SrHCF and K_2BaHCF are shown in Fig. 3*c*. While a $\delta(\text{HOH})$ signal is observed for K_2BaHCF at 1611 cm^{-1} along with $\nu(\text{OH})$ signals at 3527 cm^{-1} and 3601 cm^{-1} , no such signals were detected for Cs_2SrHCF . This absence of water was confirmed by TGA, which showed no mass loss between 30 and 400°C (Fig. S1 in the supporting information). The largest change was in the $\nu(\text{M}–\text{N})$ stretching mode, which shifted from 421 cm^{-1} $\nu(\text{Ba}–\text{N})$ to 439 cm^{-1} $\nu(\text{Sr}–\text{N})$ (Fig. 3*d*).

5. Refinement

Crystal data and details of the data collection and structure refinement methods are summarized in Table 2. The observed and calculated intensities are shown in Fig. 4 along with the difference pattern. For the refinement of $\text{Cs}_2\text{Sr}[\text{Fe}(\text{CN})_6]$, atomic positions of the $\text{Cs}_2\text{Na}[\text{Mn}(\text{CN})_6]$ phase (Ziegler *et al.*, 1989) and the given individual isotropic displacement parameters were used. All occupancies were set to unity because of the experimentally determined composition. Except for cesium, all displacement parameters were kept fixed because otherwise some became negative. The positions of the nitrogen and carbon atoms were also kept fixed. Since iron and strontium atoms are in special positions, only the lattice parameters, the position of the cesium atom and its U_{iso} value

Table 2
Experimental details.

Crystal data	
Chemical formula	$\text{Cs}_2\text{Sr}[\text{Fe}(\text{CN})_6]$
M_r	565.4
Crystal system, space group	Monoclinic, $P2_1/n$
Temperature (K)	293
a, b, c (Å)	7.6237 (2), 7.7885 (2), 10.9600 (3)
β (°)	90.4165 (19)
V (Å ³)	650.76 (4)
Z	2
Radiation type	Cu $K\alpha_1$, $\lambda = 1.540562, 1.544390$ Å
Specimen shape, size (mm)	Flat sheet, 25×25
Data collection	
Diffractometer	Panalytical XPert MPD Pro
Specimen mounting	Packed powder pellet
Data collection mode	Reflection
Scan method	Step
2θ values (°)	$2\theta_{\text{min}} = 10.023$ $2\theta_{\text{max}} = 130.010$ $2\theta_{\text{step}} = 0.017$
Refinement	
R factors and goodness of fit	$R_p = 0.031$, $R_{\text{wp}} = 0.043$, $R_{\text{exp}} = 0.025$, $R(F) = 0.101$, $\chi^2 = 2.993$
No. of parameters	11

Coordinates from an isotypic compound. Computer programs: *Data Collector* (Panalytical, 2011), *JANA2006* (Petříček *et al.*, 2014), *VESTA* (Momma & Izumi, 2011) and *publCIF* (Westrip, 2010).

were refined, together with three profile parameters. The residual electron density is about 6.06 e^{-3} at a distance of 0.71 Å from Cs.

Funding information

Funding for this research was provided by: the Center for Hierarchical Waste Forms (CHWM), an Energy Frontier Research Center funded by the U.S. Department Of Energy, Office of Basic Energy Sciences, Division of Materials Sciences and Engineering under Award DE-SC0016574.

References

- Bergerhoff, G., Berndt, M., Brandenburg, K. & Degen, T. (1999). *Acta Cryst.* **B55**, 147–156.
- Flor, G. de la, Orobengoa, D., Tasci, E., Perez-Mato, J. M. & Aroyo, M. I. (2016). *J. Appl. Cryst.* **49**, 653–664.
- Gates-Rector, S. & Blanton, T. (2019). *Powder Diffr.* **34**, 352–360.
- Gray, H. B. & Beach, N. A. (1963). *J. Am. Chem. Soc.* **85**, 2922–2927.
- Haas, P. A. (1993). *Sep. Sci. Technol.* **28**, 2479–2506.
- Kuznetsov, V. G., Popova, Z. V. & Seifer, G. B. (1970). *Russ. J. Inorg. Chem.* **15**, 1084–1088.
- Loye, H. C. zur, Besmann, T., Amoroso, J., Brinkman, K., Grandjean, A., Henager, C. H., Hu, S., Misture, S. T., Phillpot, S. R., Shustova, N. B., Wang, H., Koch, R. J., Morrison, G. & Dolgoplova, E. (2018). *Chem. Mater.* **30**, 4475–4488.
- Mimura, H., Lehto, J. & Harjula, R. (1997). *J. Nucl. Sci. Technol.* **34**, 484–489.
- Momma, K. & Izumi, F. (2011). *J. Appl. Cryst.* **44**, 1272–1276.
- Padigi, P., Goncher, G., Evans, D. & Solanki, R. (2015). *J. Power Sources*, **273**, 460–464.
- Panalytical (2011). X'Pert Data Collector. PANalytical BV, Almelo, The Netherlands.

- Paolella, A., Faure, C., Timoshevskii, V., Marras, S., Bertoni, G., Guerfi, A., Vijn, A., Armand, M. & Zaghbi, K. (2017). *J. Mater. Chem. A*, **5**, 18919–18932.
- Petríček, V., Dušek, M. & Palatinus, L. (2014). *Z. Kristallogr.* **229**, 345–352.
- Shannon, R. D. (1976). *Acta Cryst.* **A32**, 751–767.
- Slivko, T., Kuligina, T. & Zimina, G. (1988). *Russ. J. Inorg. Chem.* **33**, 1060.
- Westrip, S. P. (2010). *J. Appl. Cryst.* **43**, 920–925.
- Ziegler, B., Haegele, R. & Babel, D. (1989). *Z. Naturforsch. B*, **44**, 896–902.

supporting information

Acta Cryst. (2020). E76, 900-904 [https://doi.org/10.1107/S2056989020006660]

Crystal structure of dicaesium strontium hexacyanidoferrate(II), $\text{Cs}_2\text{Sr}[\text{Fe}(\text{CN})_6]$, from laboratory X-ray powder data

Nicolas Massoni, Mícheál P. Moloney, Agnès Grandjean, Scott T. Misture and Hans-Conrad zur Loye

Computing details

Data collection: *Data Collector* (Panalytical, 2011); cell refinement: *JANA2006* (Petříček *et al.*, 2014); data reduction: *JANA2006* (Petříček *et al.*, 2014); program(s) used to solve structure: coordinates from isotypic compound; program(s) used to refine structure: *JANA2006* (Petříček *et al.*, 2014); molecular graphics: *VESTA* (Momma & Izumi, 2011); software used to prepare material for publication: *publCIF* (Westrip, 2010).

Dicaesium strontium hexacyanidoferrate

Crystal data

$\text{Cs}_2\text{Sr}[\text{Fe}(\text{CN})_6]$

$M_r = 565.4$

Monoclinic, $P2_1/n$

$a = 7.6237$ (2) Å

$b = 7.7885$ (2) Å

$c = 10.9600$ (3) Å

$\beta = 90.4165$ (19)°

$V = 650.76$ (4) Å³

$Z = 2$

$F(000) = 504$

y

$D_x = 2.885$ Mg m⁻³

Cu $K\alpha_1$ radiation, $\lambda = 1.540562, 1.544390$ Å

$T = 293$ K

Particle morphology: plate-like

brown

flat_sheet, 25 × 25 mm

Specimen preparation: Prepared at 1873 K and 100 kPa, cooled at 30 K min⁻¹

Data collection

Panalytical XPert MPD Pro diffractometer

Radiation source: sealed X-ray tube

Specimen mounting: packed powder pellet

Data collection mode: reflection

Scan method: step

$2\theta_{\min} = 10.023^\circ$, $2\theta_{\max} = 130.010^\circ$, $2\theta_{\text{step}} = 0.017^\circ$

Refinement

$R_p = 0.031$

$R_{\text{wp}} = 0.043$

$R_{\text{exp}} = 0.025$

$R(F) = 0.101$

6881 data points

Profile function: Lorentzian

11 parameters

0 restraints

26 constraints

Weighting scheme based on measured s.u.'s (Δ/σ)_{max} = 0.012

Background function: Manual background

Special details

Refinement. The Platon test reports 21 Alerts level C. They could be gathered in three groups for explanation :
 i) 17 C-Alerts (out of 21) are "missing esd on x,y,z coordinates of N and C atoms. This is normal since these positions were not refined. Hence no esd was calculated by Jana2006.
 ii) 3 C-Alerts (out of 21) are due to a slightly larger Fourier difference density than allowed by CheckCIF. I can not enhance the quality of the data so no reduction of this value can be done.
 iii) The last C-Alert is about a "calc. and reported Sum Formula which differ. I did not find the origin of the Alert.

Fractional atomic coordinates and isotropic or equivalent isotropic displacement parameters (\AA^2)

	<i>x</i>	<i>y</i>	<i>z</i>	$U_{\text{iso}}^*/U_{\text{eq}}$
Cs	0.5080 (4)	-0.04022 (18)	0.2497 (7)	0.0410 (6)*
Sr	0	0	0.5	0.024*
Fe	0	0	0	0.019*
C1	0.0488	0.0087	0.178	0.029*
N1	0.0754	0.0169	0.2809	0.052*
C2	-0.2128	0.1444	0.022	0.03*
N2	-0.3347	0.2296	0.0368	0.048*
C3	0.1449	0.2097	-0.0251	0.029*
N3	0.2281	0.3301	-0.0406	0.046*

Atomic displacement parameters (\AA^2)

	U^{11}	U^{22}	U^{33}	U^{12}	U^{13}	U^{23}
Cs	0.0576 (17)	0.0343 (13)	0.0345 (16)	-0.016 (4)	0.0050 (17)	-0.008 (4)

Geometric parameters (\AA , $^\circ$)

Cs—C1	3.603 (3)	Sr—N3 ⁱ	2.4965 (1)
Cs—C1 ⁱ	3.628 (2)	Sr—N3 ^{vi}	2.4965 (1)
Cs—N1	3.348 (3)	Fe—C1	1.9845 (1)
Cs—N1 ⁱ	3.5232 (18)	Fe—C1 ^{vii}	1.9845 (1)
Cs—C2 ⁱⁱ	3.592 (6)	Fe—C2	1.9901 (1)
Cs—N2 ⁱⁱ	3.367 (6)	Fe—C2 ^{vii}	1.9901 (1)
Cs—C3 ⁱⁱⁱ	3.711 (5)	Fe—C3	1.9920 (1)
Cs—N3 ⁱⁱⁱ	3.274 (6)	Fe—C3 ^{vii}	1.9920 (1)
Sr—N1	2.4767 (1)	C1—N1	1.1462 (1)
Sr—N1 ^{iv}	2.4767 (1)	C2—N2	1.1543 (1)
Sr—N2 ^v	2.4857 (1)	C3—N3	1.1455 (1)
Sr—N2 ⁱⁱⁱ	2.4857 (1)		
Cs ⁱ —Cs—Cs ^{viii}	89.42 (6)	N1—Cs—N3 ⁱⁱⁱ	111.23 (16)
Cs ⁱ —Cs—Cs ^{ix}	88.75 (4)	N1 ⁱ —Cs—C2 ⁱⁱ	115.67 (16)
Cs ⁱ —Cs—Cs ^x	178.16 (6)	N1 ⁱ —Cs—N2 ⁱⁱ	127.6 (2)
Cs ⁱ —Cs—Cs ^{xi}	94.04 (12)	N1 ⁱ —Cs—C3 ⁱⁱⁱ	142.4 (2)
Cs ⁱ —Cs—Cs ^{xii}	93.31 (12)	N1 ⁱ —Cs—N3 ⁱⁱⁱ	130.34 (17)
Cs ⁱ —Cs—Sr	57.71 (7)	C2 ⁱⁱ —Cs—N2 ⁱⁱ	18.74 (3)
Cs ⁱ —Cs—Sr ⁱⁱ	128.17 (12)	C2 ⁱⁱ —Cs—C3 ⁱⁱⁱ	91.10 (5)
Cs ⁱ —Cs—Sr ⁱ	55.62 (7)	C2 ⁱⁱ —Cs—N3 ⁱⁱⁱ	89.11 (6)

Cs ⁱ —Cs—Sr ^{viii}	125.77 (11)	N2 ⁱⁱ —Cs—C3 ⁱⁱⁱ	85.88 (4)
Cs ⁱ —Cs—C1	52.06 (4)	N2 ⁱⁱ —Cs—N3 ⁱⁱⁱ	89.50 (5)
Cs ⁱ —Cs—C1 ⁱ	39.87 (4)	C3 ⁱⁱⁱ —Cs—N3 ⁱⁱⁱ	17.47 (3)
Cs ⁱ —Cs—N1	52.61 (4)	Cs ^{xiii} —Sr—Cs	108.15 (11)
Cs ⁱ —Cs—N1 ⁱ	35.27 (4)	Cs ^{xiii} —Sr—Cs ⁱ	67.33 (6)
Cs ⁱ —Cs—C2 ⁱⁱ	135.00 (18)	Cs ^{xiii} —Sr—Cs ^{viii}	71.79 (7)
Cs ⁱ —Cs—N2 ⁱⁱ	134.15 (18)	Cs ^{xiii} —Sr—Cs ^{iv}	71.85 (11)
Cs ⁱ —Cs—C3 ⁱⁱⁱ	133.13 (17)	Cs ^{xiii} —Sr—Cs ^{xii}	180
Cs ⁱ —Cs—N3 ⁱⁱⁱ	135.35 (19)	Cs ^{xiii} —Sr—Cs ^{xiv}	108.21 (7)
Cs ^{viii} —Cs—Cs ^{ix}	178.16 (6)	Cs ^{xiii} —Sr—Cs ^{vi}	112.67 (6)
Cs ^{viii} —Cs—Cs ^x	88.75 (4)	Cs ^{xiii} —Sr—N1	67.84 (8)
Cs ^{viii} —Cs—Cs ^{xi}	84.87 (11)	Cs ^{xiii} —Sr—N1 ^{iv}	112.16 (8)
Cs ^{viii} —Cs—Cs ^{xii}	84.16 (11)	Cs ^{xiii} —Sr—N2 ^v	55.97 (3)
Cs ^{viii} —Cs—Sr	51.21 (7)	Cs ^{xiii} —Sr—N2 ⁱⁱⁱ	124.03 (3)
Cs ^{viii} —Cs—Sr ⁱⁱ	121.54 (11)	Cs ^{xiii} —Sr—N3 ⁱ	137.39 (4)
Cs ^{viii} —Cs—Sr ⁱ	123.59 (12)	Cs ^{xiii} —Sr—N3 ^{vi}	42.61 (4)
Cs ^{viii} —Cs—Sr ^{viii}	53.50 (6)	Cs—Sr—Cs ⁱ	68.79 (6)
Cs ^{viii} —Cs—C1	40.22 (4)	Cs—Sr—Cs ^{viii}	73.18 (7)
Cs ^{viii} —Cs—C1 ⁱ	126.52 (9)	Cs—Sr—Cs ^{iv}	180
Cs ^{viii} —Cs—N1	37.42 (4)	Cs—Sr—Cs ^{xii}	71.85 (11)
Cs ^{viii} —Cs—N1 ⁱ	124.14 (8)	Cs—Sr—Cs ^{xiv}	106.82 (7)
Cs ^{viii} —Cs—C2 ⁱⁱ	98.28 (9)	Cs—Sr—Cs ^{vi}	111.21 (6)
Cs ^{viii} —Cs—N2 ⁱⁱ	79.54 (8)	Cs—Sr—N1	41.51 (8)
Cs ^{viii} —Cs—C3 ⁱⁱⁱ	73.00 (7)	Cs—Sr—N1 ^{iv}	138.49 (8)
Cs ^{viii} —Cs—N3 ⁱⁱⁱ	90.47 (9)	Cs—Sr—N2 ^v	105.29 (4)
Cs ^{ix} —Cs—Cs ^x	93.09 (6)	Cs—Sr—N2 ⁱⁱⁱ	74.71 (4)
Cs ^{ix} —Cs—Cs ^{xi}	95.39 (13)	Cs—Sr—N3 ⁱ	52.52 (6)
Cs ^{ix} —Cs—Cs ^{xii}	95.81 (13)	Cs—Sr—N3 ^{vi}	127.48 (6)
Cs ^{ix} —Cs—Sr	127.44 (12)	Cs ⁱ —Sr—Cs ^{viii}	109.57 (11)
Cs ^{ix} —Cs—Sr ⁱⁱ	59.69 (7)	Cs ⁱ —Sr—Cs ^{iv}	111.21 (6)
Cs ^{ix} —Cs—Sr ⁱ	55.27 (7)	Cs ⁱ —Sr—Cs ^{xii}	112.67 (6)
Cs ^{ix} —Cs—Sr ^{viii}	127.94 (12)	Cs ⁱ —Sr—Cs ^{xiv}	70.43 (11)
Cs ^{ix} —Cs—C1	138.10 (8)	Cs ⁱ —Sr—Cs ^{vi}	180
Cs ^{ix} —Cs—C1 ⁱ	51.68 (4)	Cs ⁱ —Sr—N1	61.18 (7)
Cs ^{ix} —Cs—N1	140.75 (6)	Cs ⁱ —Sr—N1 ^{iv}	118.82 (7)
Cs ^{ix} —Cs—N1 ⁱ	54.06 (4)	Cs ⁱ —Sr—N2 ^v	36.60 (5)
Cs ^{ix} —Cs—C2 ⁱⁱ	83.13 (9)	Cs ⁱ —Sr—N2 ⁱⁱⁱ	143.40 (5)
Cs ^{ix} —Cs—N2 ⁱⁱ	101.85 (11)	Cs ⁱ —Sr—N3 ⁱ	70.10 (5)
Cs ^{ix} —Cs—C3 ⁱⁱⁱ	108.22 (12)	Cs ⁱ —Sr—N3 ^{vi}	109.90 (5)
Cs ^{ix} —Cs—N3 ⁱⁱⁱ	90.74 (10)	Cs ^{viii} —Sr—Cs ^{iv}	106.82 (7)
Cs ^x —Cs—Cs ^{xi}	85.93 (12)	Cs ^{viii} —Sr—Cs ^{xii}	108.21 (7)
Cs ^x —Cs—Cs ^{xii}	86.37 (12)	Cs ^{viii} —Sr—Cs ^{xiv}	180
Cs ^x —Cs—Sr	120.84 (11)	Cs ^{viii} —Sr—Cs ^{vi}	70.43 (11)
Cs ^x —Cs—Sr ⁱⁱ	52.95 (7)	Cs ^{viii} —Sr—N1	51.05 (8)
Cs ^x —Cs—Sr ⁱ	125.72 (13)	Cs ^{viii} —Sr—N1 ^{iv}	128.95 (8)
Cs ^x —Cs—Sr ^{viii}	52.97 (6)	Cs ^{viii} —Sr—N2 ^v	124.75 (7)
Cs ^x —Cs—C1	126.21 (7)	Cs ^{viii} —Sr—N2 ⁱⁱⁱ	55.25 (7)
Cs ^x —Cs—C1 ⁱ	141.80 (10)	Cs ^{viii} —Sr—N3 ⁱ	122.47 (4)

Cs ^x —Cs—N1	125.56 (5)	Cs ^{viii} —Sr—N3 ^{vi}	57.53 (4)
Cs ^x —Cs—N1 ⁱ	146.56 (9)	Cs ^{iv} —Sr—Cs ^{xii}	108.15 (11)
Cs ^x —Cs—C2 ⁱⁱ	45.51 (8)	Cs ^{iv} —Sr—Cs ^{xiv}	73.18 (7)
Cs ^x —Cs—N2 ⁱⁱ	45.53 (9)	Cs ^{iv} —Sr—Cs ^{vi}	68.79 (6)
Cs ^x —Cs—C3 ⁱⁱⁱ	46.01 (8)	Cs ^{iv} —Sr—N1	138.49 (8)
Cs ^x —Cs—N3 ⁱⁱⁱ	44.55 (9)	Cs ^{iv} —Sr—N1 ^{iv}	41.51 (8)
Cs ^{xi} —Cs—Cs ^{xiii}	166.72 (4)	Cs ^{iv} —Sr—N2 ^v	74.71 (4)
Cs ^{xi} —Cs—Sr	123.46 (9)	Cs ^{iv} —Sr—N2 ⁱⁱⁱ	105.29 (4)
Cs ^{xi} —Cs—Sr ⁱⁱ	126.26 (10)	Cs ^{iv} —Sr—N3 ⁱ	127.48 (6)
Cs ^{xi} —Cs—Sr ⁱ	59.14 (9)	Cs ^{iv} —Sr—N3 ^{vi}	52.52 (6)
Cs ^{xi} —Cs—Sr ^{viii}	50.43 (7)	Cs ^{xii} —Sr—Cs ^{xiv}	71.79 (7)
Cs ^{xi} —Cs—C1	75.93 (12)	Cs ^{xii} —Sr—Cs ^{vi}	67.33 (6)
Cs ^{xi} —Cs—C1 ⁱ	108.98 (13)	Cs ^{xii} —Sr—N1	112.16 (8)
Cs ^{xi} —Cs—N1	94.11 (14)	Cs ^{xii} —Sr—N1 ^{iv}	67.84 (8)
Cs ^{xi} —Cs—N1 ⁱ	90.80 (13)	Cs ^{xii} —Sr—N2 ^v	124.03 (3)
Cs ^{xi} —Cs—C2 ⁱⁱ	43.39 (9)	Cs ^{xii} —Sr—N2 ⁱⁱⁱ	55.97 (3)
Cs ^{xi} —Cs—N2 ⁱⁱ	41.07 (9)	Cs ^{xii} —Sr—N3 ⁱ	42.61 (4)
Cs ^{xi} —Cs—C3 ⁱⁱⁱ	125.88 (9)	Cs ^{xii} —Sr—N3 ^{vi}	137.39 (4)
Cs ^{xi} —Cs—N3 ⁱⁱⁱ	130.40 (11)	Cs ^{xiv} —Sr—Cs ^{vi}	109.57 (11)
Cs ^{xii} —Cs—Sr	52.97 (8)	Cs ^{xiv} —Sr—N1	128.95 (8)
Cs ^{xii} —Cs—Sr ⁱⁱ	55.18 (8)	Cs ^{xiv} —Sr—N1 ^{iv}	51.05 (8)
Cs ^{xii} —Cs—Sr ⁱ	133.85 (9)	Cs ^{xiv} —Sr—N2 ^v	55.25 (7)
Cs ^{xii} —Cs—Sr ^{viii}	116.50 (7)	Cs ^{xiv} —Sr—N2 ⁱⁱⁱ	124.75 (7)
Cs ^{xii} —Cs—C1	100.15 (13)	Cs ^{xiv} —Sr—N3 ⁱ	57.53 (4)
Cs ^{xii} —Cs—C1 ⁱ	83.65 (13)	Cs ^{xiv} —Sr—N3 ^{vi}	122.47 (4)
Cs ^{xii} —Cs—N1	81.64 (13)	Cs ^{vi} —Sr—N1	118.82 (7)
Cs ^{xii} —Cs—N1 ⁱ	101.55 (14)	Cs ^{vi} —Sr—N1 ^{iv}	61.18 (7)
Cs ^{xii} —Cs—C2 ⁱⁱ	131.46 (10)	Cs ^{vi} —Sr—N2 ^v	143.40 (5)
Cs ^{xii} —Cs—N2 ⁱⁱ	128.90 (10)	Cs ^{vi} —Sr—N2 ⁱⁱⁱ	36.60 (5)
Cs ^{xii} —Cs—C3 ⁱⁱⁱ	43.02 (8)	Cs ^{vi} —Sr—N3 ⁱ	109.90 (5)
Cs ^{xii} —Cs—N3 ⁱⁱⁱ	42.36 (10)	Cs ^{vi} —Sr—N3 ^{vi}	70.10 (5)
Sr—Cs—Sr ⁱⁱ	108.15 (15)	N1—Sr—N1 ^{iv}	180
Sr—Cs—Sr ⁱ	113.18 (5)	N1—Sr—N2 ^v	90.4970 (12)
Sr—Cs—Sr ^{viii}	104.58 (4)	N1—Sr—N2 ⁱⁱⁱ	89.5030 (12)
Sr—Cs—C1	47.71 (5)	N1—Sr—N3 ⁱ	90.1559 (18)
Sr—Cs—C1 ⁱ	80.76 (9)	N1—Sr—N3 ^{vi}	89.8441 (18)
Sr—Cs—N1	29.36 (6)	N1 ^{iv} —Sr—N2 ^v	89.5030 (12)
Sr—Cs—N1 ⁱ	88.41 (8)	N1 ^{iv} —Sr—N2 ⁱⁱⁱ	90.4970 (12)
Sr—Cs—C2 ⁱⁱ	149.38 (7)	N1 ^{iv} —Sr—N3 ⁱ	89.8441 (18)
Sr—Cs—N2 ⁱⁱ	130.69 (6)	N1 ^{iv} —Sr—N3 ^{vi}	90.1559 (18)
Sr—Cs—C3 ⁱⁱⁱ	78.33 (11)	N2 ^v —Sr—N2 ⁱⁱⁱ	180
Sr—Cs—N3 ⁱⁱⁱ	88.72 (14)	N2 ^v —Sr—N3 ⁱ	89.952 (2)
Sr ⁱⁱ —Cs—Sr ⁱ	114.82 (5)	N2 ^v —Sr—N3 ^{vi}	90.048 (2)
Sr ⁱⁱ —Cs—Sr ^{viii}	105.80 (4)	N2 ⁱⁱⁱ —Sr—N3 ⁱ	90.048 (2)
Sr ⁱⁱ —Cs—C1	154.37 (18)	N2 ⁱⁱⁱ —Sr—N3 ^{vi}	89.952 (2)
Sr ⁱⁱ —Cs—C1 ⁱ	91.92 (10)	N3 ⁱ —Sr—N3 ^{vi}	180
Sr ⁱⁱ —Cs—N1	136.3 (2)	C1—Fe—C1 ^{vii}	180
Sr ⁱⁱ —Cs—N1 ⁱ	105.47 (9)	C1—Fe—C2	90.5021 (17)

Sr ⁱⁱ —Cs—C2 ⁱⁱ	84.45 (6)	C1—Fe—C2 ^{vii}	89.4979 (17)
Sr ⁱⁱ —Cs—N2 ⁱⁱ	94.42 (6)	C1—Fe—C3	90.4341 (12)
Sr ⁱⁱ —Cs—C3 ⁱⁱⁱ	48.54 (6)	C1—Fe—C3 ^{vii}	89.5659 (12)
Sr ⁱⁱ —Cs—N3 ⁱⁱⁱ	31.08 (4)	C1 ^{vii} —Fe—C2	89.4979 (17)
Sr ⁱ —Cs—Sr ^{viii}	109.57 (15)	C1 ^{vii} —Fe—C2 ^{vii}	90.5021 (17)
Sr ⁱ —Cs—C1	86.72 (10)	C1 ^{vii} —Fe—C3	89.5660 (12)
Sr ⁱ —Cs—C1 ⁱ	50.37 (4)	C1 ^{vii} —Fe—C3 ^{vii}	90.4341 (12)
Sr ⁱ —Cs—N1	99.12 (9)	C2—Fe—C2 ^{vii}	180
Sr ⁱ —Cs—N1 ⁱ	33.14 (5)	C2—Fe—C3	90.387 (2)
Sr ⁱ —Cs—C2 ⁱⁱ	84.36 (13)	C2—Fe—C3 ^{vii}	89.613 (2)
Sr ⁱ —Cs—N2 ⁱⁱ	94.50 (16)	C2 ^{vii} —Fe—C3	89.613 (2)
Sr ⁱ —Cs—C3 ⁱⁱⁱ	163.24 (9)	C2 ^{vii} —Fe—C3 ^{vii}	90.387 (2)
Sr ⁱ —Cs—N3 ⁱⁱⁱ	145.89 (8)	C3—Fe—C3 ^{vii}	180
Sr ^{viii} —Cs—C1	77.56 (8)	Cs—C1—Cs ^{viii}	99.91 (7)
Sr ^{viii} —Cs—C1 ⁱ	158.40 (18)	Cs—C1—Fe	112.69 (12)
Sr ^{viii} —Cs—N1	86.35 (7)	Cs—C1—N1	68.07 (12)
Sr ^{viii} —Cs—N1 ⁱ	140.12 (19)	Cs ^{viii} —C1—Fe	103.06 (12)
Sr ^{viii} —Cs—C2 ⁱⁱ	44.81 (5)	Cs ^{viii} —C1—N1	75.62 (12)
Sr ^{viii} —Cs—N2 ⁱⁱ	26.11 (2)	Fe—C1—N1	178.6228 (6)
Sr ^{viii} —Cs—C3 ⁱⁱⁱ	77.49 (3)	Cs—N1—Cs ^{viii}	107.31 (6)
Sr ^{viii} —Cs—N3 ⁱⁱⁱ	88.16 (4)	Cs—N1—Sr	109.13 (13)
C1—Cs—C1 ⁱ	91.87 (6)	Cs—N1—C1	93.41 (13)
C1—Cs—N1	18.52 (2)	Cs ^{viii} —N1—Sr	95.82 (12)
C1—Cs—N1 ⁱ	84.74 (7)	Cs ^{viii} —N1—C1	86.01 (12)
C1—Cs—C2 ⁱⁱ	112.70 (17)	Sr—N1—C1	155.5560 (16)
C1—Cs—N2 ⁱⁱ	97.66 (14)	Cs ^{xiii} —C2—Fe	110.22 (4)
C1—Cs—C3 ⁱⁱⁱ	109.87 (10)	Cs ^{xiii} —C2—N2	69.56 (4)
C1—Cs—N3 ⁱⁱⁱ	126.34 (13)	Fe—C2—N2	178.6331 (10)
C1 ⁱ —Cs—N1	89.26 (7)	Cs ^{xiii} —N2—Sr ^{xv}	117.29 (5)
C1 ⁱ —Cs—N1 ⁱ	18.369 (10)	Cs ^{xiii} —N2—C2	91.71 (5)
C1 ⁱ —Cs—C2 ⁱⁱ	127.70 (13)	Sr ^{xv} —N2—C2	150.6891 (7)
C1 ⁱ —Cs—N2 ⁱⁱ	143.06 (18)	Cs ^{xvi} —C3—Fe	120.47 (5)
C1 ⁱ —Cs—C3 ⁱⁱⁱ	124.0 (2)	Cs ^{xvi} —C3—N3	59.13 (5)
C1 ⁱ —Cs—N3 ⁱⁱⁱ	113.08 (18)	Fe—C3—N3	179.4092 (8)
N1—Cs—N1 ⁱ	87.85 (6)	Cs ^{xvi} —N3—Sr ^{viii}	106.31 (4)
N1—Cs—C2 ⁱⁱ	127.37 (16)	Cs ^{xvi} —N3—C3	103.40 (4)
N1—Cs—N2 ⁱⁱ	110.12 (12)	Sr ^{viii} —N3—C3	150.1635 (8)
N1—Cs—C3 ⁱⁱⁱ	96.46 (12)		

Symmetry codes: (i) $-x+1/2, y-1/2, -z+1/2$; (ii) $x+1, y, z$; (iii) $x+1/2, -y+1/2, z+1/2$; (iv) $-x, -y, -z+1$; (v) $-x-1/2, y-1/2, -z+1/2$; (vi) $x-1/2, -y+1/2, z+1/2$; (vii) $-x, -y, -z$; (viii) $-x+1/2, y+1/2, -z+1/2$; (ix) $-x+3/2, y-1/2, -z+1/2$; (x) $-x+3/2, y+1/2, -z+1/2$; (xi) $-x+1, -y, -z$; (xii) $-x+1, -y, -z+1$; (xiii) $x-1, y, z$; (xiv) $x-1/2, -y-1/2, z+1/2$; (xv) $-x-1/2, y+1/2, -z+1/2$; (xvi) $x-1/2, -y+1/2, z-1/2$.